Distribution Category:
Magnetic Fusion Energy
(UC-20)

ANL/FPP/TM-175

ANL/FPP/TM--175

DE83 015751

ARGONNE NATIONAL LABORATORY
9700 South Cass Avenue
Argonne, Illinois 60439

PUMPED-LIMITER STUDY FOR ALCATOR DCT

by

J. N. Brooks, R. F. Mattas, Y. S. Cha,
A. M. Hassanein, and S. Majumdar

Fusion Power Program

DISCLAIMER

June 1983

TABLE OF CONTENTS

LIST OF FIGURES

LIST OF TABLES

PUMPED LIMITER STUDY FOR ALCATOR DCT

By

J. N. Brooks and R. F. Mattas

Y. S. Cha, A. M. Hassanein, and S. Majumdar

ABSTRACT

A study was performed for a pumped limiter design for the proposed Alcator DCT device. The study focused on reactor relevant issues. The main issues examined were configuration, surface erosion, thermal hydraulics, and the choice of structural and surface materials. A bottom, flat limiter, with a copper alloy substrate, seems to be a reasonable design and should provide an opportunity to test high power and particle loadings. Carbon is recommended as a surface material if acceptable redeposition properties can be demonstrated.

1.0 INTRODUCTION

This report discusses some of the issues associated with the design and operation of a pumped limiter for the proposed Alcator DCT device.[1] The limiter configuration analyzed was a continuous, flat limiter, located at the bottom of the plasma chamber. Most of the issues discussed here would also apply to other limiter configurations or to a divertor collector plate.

The Alcator DCT device appears to offer an opportunity to study many of the key impurity control issues associated with future tokamak reactors, e.g., high heat and particle loads, effects of disruptions, erosion/redeposition, and edge temperature characterization and control. At the same time, the impurity control system requirements are obviously easier because of the low duty factor and absence of radiation damage. The intent of this brief study was to examine some of these critical issues as they affect the design of a pumped limiter system for Alcator DCT. The areas covered here are erosion/redeposition, disruption induced erosion, choice of materials, thermal hydraulics and stress analysis, and the overall limiter lifetime. Based on this analysis, we have made a number of initial recommendations for the pumped limiter design (see Section 8.0).

2.0 CONFIGURATION

In general, the main pumped limiter configuration choices are as follows: location (bottom, top, or midplane), number of limiter locations (one or two), shape (curved or flat), number of leading edges (one or two), and limiter segmentation (quasi-continuous or discontinuous). The main tradeoffs among these configurations are heat load, pumping efficiency, fabricability, and ease of maintenance. Based on an initial assessment of these considerations, a bottom, flat, single edge, continuous limiter seems to be a good choice for Alcator DCT. Such a limiter would be made of a number of segments, but these would be close enough so that the limiter would be effectively continuous, from the standpoint of the plasma flux.

There are two major advantages to this configuration: (1) a flat shape is simple to fabricate and (2) the limiter can be moved in or out in major radius to compensate for changes in scrapeoff e-folding distances. Also, this design is reasonably "reactor relevant". The main disadvantages to this configuration are (1) higher peak heat flux (relative to a curved shape) and (2) less particle pumping (relative to a 2-leading edge design). These disadvantages, however, are not critical to the Alcator DCT design. Also, there may be possible problems with diagnostic access, with a continuous design,[2] and this needs further examination.

3.0 EROSION/REDEPOSITION

Erosion by sputtering is one of the most critical issues facing impurity control systems of future tokamak reactors. Sputtering erosion will not be significant in Alcator DCT, or any near term device, simply because of the small operating time. However, contamination of the plasma and the achieving of a long pulse ($\sim$ 1000 s) is critically dependent on erosion/redeposition. In addition, even the small layers of redeposited material formed can be useful for research purposes.

Erosion/redeposition calculations were made for a bottom limiter design using the REDEP code.[3,4] Parameters were chosen from a combination of the Alcator DCT design parameters[5] where available, and scaling from the INTOR design.[6] In particular, charge exchange neutral sputtering was scaled from

the DEGAS code results for INTOR, for an assumed charge exchange power of 1.0 MW to the limiter. An edge temperature of 150 eV was used in the calculations. Parameters for the calculations are shown in Table 3-1.

Table 3-1
Parameters Used for Erosion/Redeposition Calculations

Major Radius, R	2 M
Minor Radius, a	0.4 M
Triangularity, D	0.2
System	Bottom Pumped Limiter ~ 32 cm Wide
Limiter Area	~ 4 m^2
Coating Material	Carbon, Beryllium
Transport Power to Limiter, P_{TR}	5 MW
cx Power to Limiter, P_{cx}	1 MW
Proton Current to Limiter, I_{p+}	4.3×10^{22} s^{-1}
Plasma Edge Temperature	150 eV
Plasma Edge Density	2.5×10^{19} m^{-3}
Scrapeoff Density e-folding Distance, δ_N	1.875 cm
Scrapeoff Temperature e-folding Distance, δ_T	1.875 cm
Fraction of Particles Entering Slot Region	~ 8%

Figure 3-1 shows the heat and particle fluxes to the limiter and Fig. 3-2 shows the sputter rates and net growth rate for a carbon coating. The limiter, shown schematically in Fig. 3-1, is designed to be inserted from the inner tokamak bore, with the leading edge extending out in major radius. A pump duct (not shown) would be located between the leading edge and the first wall. (Limiter points are defined as pt 2 to pt 26 with pts 2-20 constituting half of the front face and pts 21-26 constituting the leading edge.) Except for the leading edge, the limiter loads and sputtering are approximately symetric about the midpoint (pt. 2) and so only the right hand side results are plotted.

As shown, the surface heat flux peaks at a value of 2 MW/m^2, a high but tolerable value. Leading edge loading is about half of this value. These

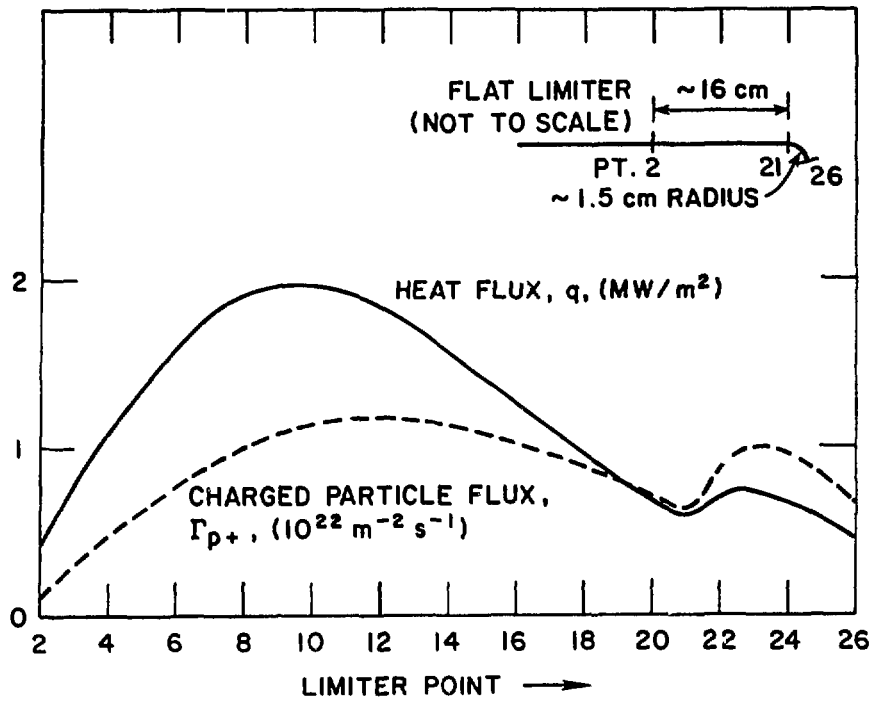

Fig. 3-1. Heat and particle loads on the reference limiter.

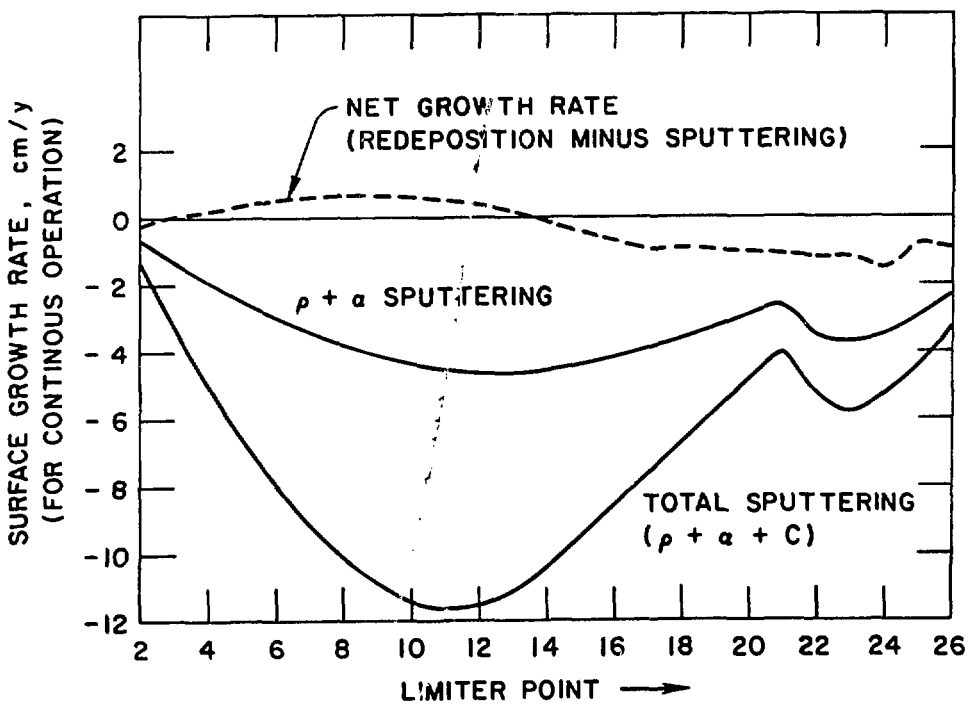

Fig. 3-2. Erosion/redeposition of a carbon limiter coating at a 150 eV edge temperature.

values are of course subject to uncertainties in the edge conditions. (For values of $\delta_N = \delta_T = 1.0$ cm, heat flux peaks at 2.6 MW/m^2.) In the erosion/redeposition calculation shown, the gross erosion rate due to proton sputtering (charged and neutral) plus a small helium component (~ 5%) peaks at about 5 cm/yr. Physical sputtering only is assumed, i.e., no chemical sputtering is included. The total gross sputtering rate, including self-sputtering peaks at ~ 12 cm/yr. Fortunately, the net growth rate is much smaller, with a small growth rate predicted over about half the limiter and a small erosion rate over the other half. The scrapeoff shielding efficiency for this case, defined as one minus the ratio of carbon atoms reaching the plasma to carbon atoms sputtered, is 78%. Thus, the net sputter rate to the plasma is only ~ 1/5 of the gross rate, due to ionization and return along field lines, in the scrapeoff zone. The effective sputtering coefficient, defined as the ratio of carbon atoms reaching the plasma to charged protons hitting the limiter is 0.0062. The maximum average carbon concentration in the plasma is this value. The value of carbon concentration in the plasma center would probably be much smaller than this value.

This calculation makes an important assumption; that redeposited carbon ions stick to the carbon surface, forming a stable surface layer. As discussed later, the sticking probabilility of carbon on carbon needs experimental assessment. A REDEP calculation made using a zero sticking probability shows that carbon builds up indefinitely in the plasma. Thus, a carbon coating is acceptable only if the redeposited particles stick. Another concern with carbon is chemical sputtering, which can be ~ 10 times higher than physical sputtering. As discussed later, it appears possible to avoid chemical sputtering in Alcator DCT, by limiting the surface temperature. Beryllium, for which the integrity of the redeposited layer is considered more certain, behaves similarly to the results shown in Fig. 3-2 and is thus acceptable, from an erosion standpoint.

4.0 DISRUPTIONS

Erosion during disruptions is expected to be a major life limiting mechanism for Alcator-DCT. The assumed disruption conditions are shown in Table 4-1. The disruption is divided into two segments - a thermal and a current quench. During the thermal quench, two thirds of the internal plasma

Table 4-1
Nominal Alcator DCT Disruption Conditions

Thermal Quench	
Time	1 ms
Energy to Limiter	2 MJ
Limiter Area	4 m^2
Disruption Peaking Factor	2.5
Peak Energy Density	125 J/cm^2
Current Quench	
Time	5 ms
Energy	1 MJ
Area Coverage	8 m^2
Disruption Peaking Factor	2.5
Peak Energy Density	31 J/cm^2

Table 4-2
Energy Densities Required for Onset of Melting or Vaporization* (8)

Material	Energy Density (J/cm^2)
Stainless Steel	80
Be	100
Mo	280
W	360
C	300
SiC	270
BeO	~100

* 5 ms disruption time.

energy (3 MJ) is assumed to strike the limiter, and during the current quench, a magnetic energy of 1 MJ[7] is assumed to strike 20% of the first wall area (inboard, top, or bottom). The energy densities for both segments of the disruption are low compared with larger devices such as INTOR.[8] Since there are uncertainties in the disruption energy densities, the vaporization and melting thicknesses have been calculated parametrically.

The vaporization and melt layer thicknesses have been calculated using a model by Hassanein.[9] The calculated losses for a 1 ms disruption are shown in Figs. 4-1 and 4-2 for candidate limiter surface materials. Both Be and BeO are predicted to melt for the nominal disruption energy density of 125 J/cm^2 with Be having the thicker melt layer (~ 45 μm). Both C and SiC are predicted to experience no material losses for the nominal disruption conditions and therefore they are preferred. For the current quench, no material losses are expected from any of the candidates. As shown in Table 4-2, the energy densities required for the onset of melting or vaporization are greater than twice the peak energy density. The material losses for the nominal disruption conditions appear to be reasonable, but more experimental and analytical effort is required to reduce the uncertainties in the disruption parameters.

5.0 MATERIALS

The candidate materials for impurity control fall into two categories - plasma side materials and heat sink materials. Plasma side materials are selected primarily for their erosion behavior from sputtering and disruptions, and heat sink materials are selected primarily for their mechanical strength, thermophysical properties, and fabricability. In general, a single material cannot serve as both the plasma side material and heat sink material. Candidate plasma side materials are C, Be, BeO, SiC, W, and Ta, and the candidate heat sink materials are copper alloys. This section will briefly review the key considerations for these materials. An extensive assessment of impurity control materials has recently been completed, and additional information can be found in reference 8.

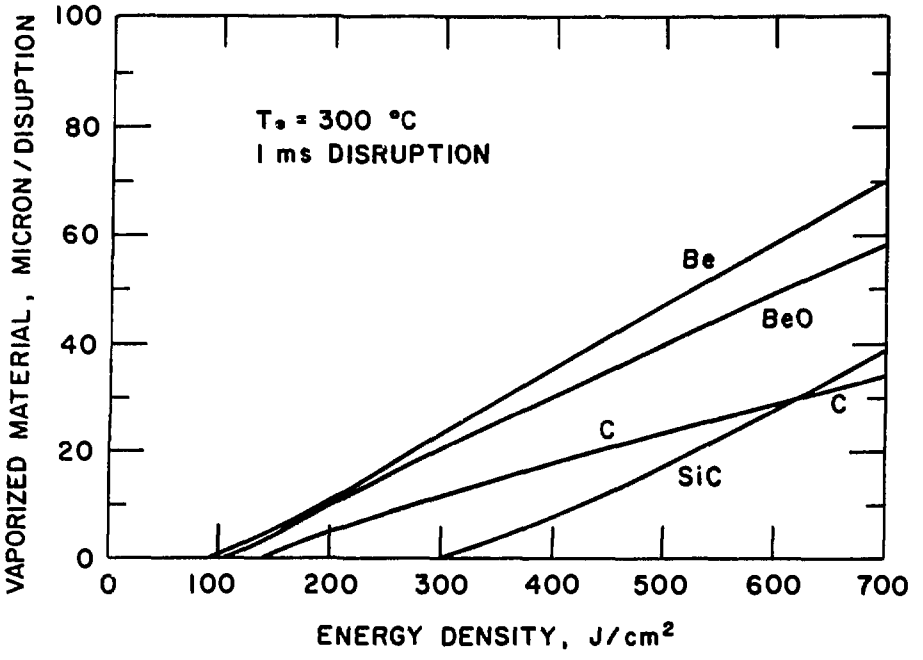

Fig. 4-1. Vaporization thickness as a function of energy density for a 1 ms disruption.

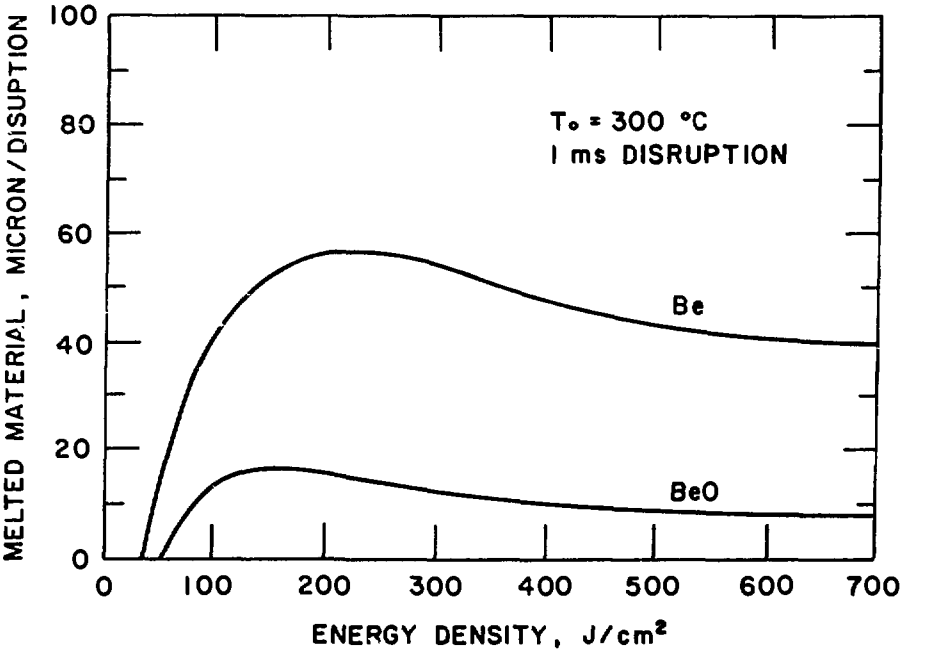

Fig. 4-2. Melt layer thickness as a function of energy density for a 1 ms disruption.

5.1 Plasma Side Materials

A summary of the favorable and unfavorable characteristics of plasma side materials is presented in Table 5-1. The key considerations are physical and chemical sputtering, response to disruptions (physical properties), availability, and safety.

The sputtering characteristics of these materials determine the plasma edge conditions where they may be used. The low-Z materials, Be, BeO, and C, can be utilized at all plasma edge temperatures since self sputtering is always less than unity. SiC appears to be a borderline case with the predicted C sputtering always less than unity but with the predicted SiC sputtering sometimes exceeding unity.[8] High-Z materials are particularly attractive at low plasma edge temperatures where the DT sputtering is close to zero. However, self sputtering exceeds unity at particle energies $\gtrsim$ 700 eV. Experimental and theoretical sputtering curves for Be, SiC, and W are shown in Figs. 5-1 to 5-3, respectively. The physical sputtering of graphite and BeO is similar to the sputtering of Be, and the physical sputtering of Ta is similar to the sputtering of W.

The primary concern for graphite is chemical sputtering. Recent experimental data is presented in Fig. 5-4.[10] Temperature dependant sputtering is observed at medium and high temperatures indicating that low temperatures ($\lesssim$ 400°C) are necessary to avoid accelerated sputtering. Another concern with graphite is the form of redeposited material. It is possible that graphite may redeposit as amorphous material in which case the properties would be considerably different from the original crystalline structure.

The primary issue for Be and BeO is the chemical toxicity. Since this issue has a significant impact on the maintainabilty of Alcator DCT, the precautions required in using Be containing material will be described. The major health concern in using Be products is berylliosis of the lungs, and therefore the precautions taken are mainly to eliminate the possibility of Be inhalation. Other precautions are taken with soluble salts of Be which can result in a dermatitus if allowed to contact the skin. In order to prevent inhalation of Be, the American Conference of Government Industrial Hygienists (ACHIF) has established a maximum allowable concentration of 2 $\mu g/m^3$ averaged over an 8 h day, and a maximum allowable concentration of 25 $\mu g/m^3$ for brief exposures.[11,12] The non-occupational exposure limit is 0.01 $\mu g/m^3$ as an

Table 5-1
Surface Material Trade-offs

Material	Favorable Characteristics	Limiting Features
Be	Self sputtering < 1 at all energies No chemical sputtering High thermal conductivity Fabrication experience	Melt layer formation during disruptions Chemical toxicity
BeO	Self sputtering < 1 at all energies High thermal conductivity No chemical sputtering	Chemical toxicity Limited technology base Melt layer formation during disruptions Uncertain stoichiometry of sputtered surface
C	Low cost, readily available Extensive database No melting during disruptions Thermal shock resistance Sputtering < 1 at all energies	Chemical sputtering Characteristics of redeposited materials
SiC	Low cost readily available No melting during disruptions Extensive database	Low thermal conductivity Chemical sputtering? Self sputtering > 1 possible Uncertain stoichiometry of sputtered surface
W	Low DT sputtering at low energies Good resistance to disruptions No chemical sputtering High thermal conductance	Difficult fabrication Self sputtering > 1 at $E \gtrsim 700$ eV High-Z impurity
Ta	Low DT sputtering at low energies Good resistance to disruptions No chemical sputtering High thermal conductivity	Self sputtering > 1 at $E \gtrsim 700$ eV High-Z impurity

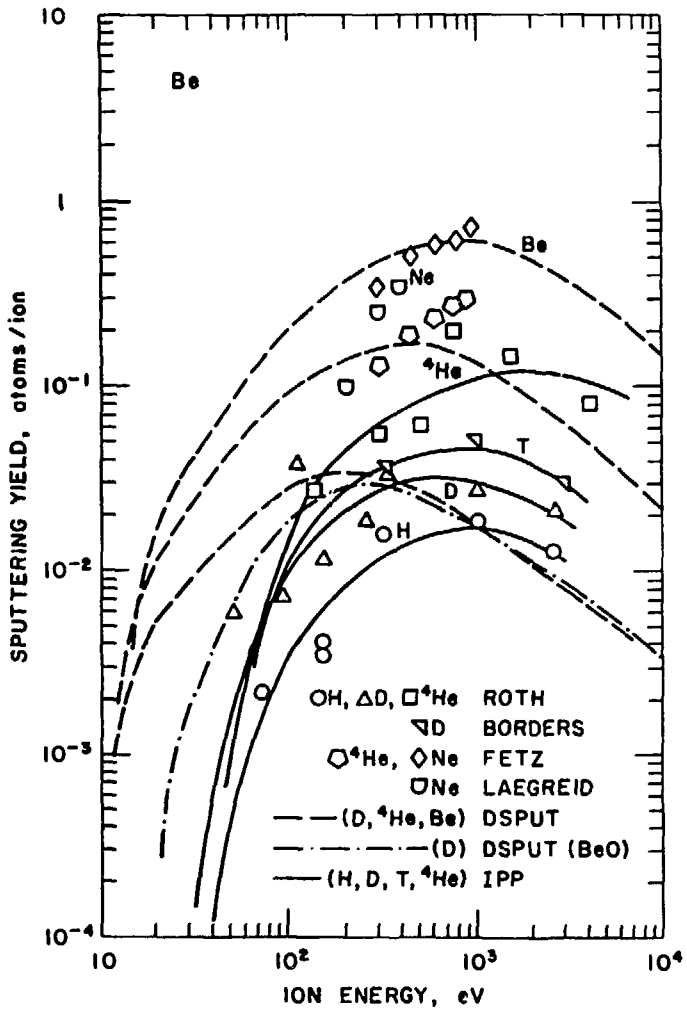

Fig. 5-1. Energy-dependent physical sputtering yields for Be.

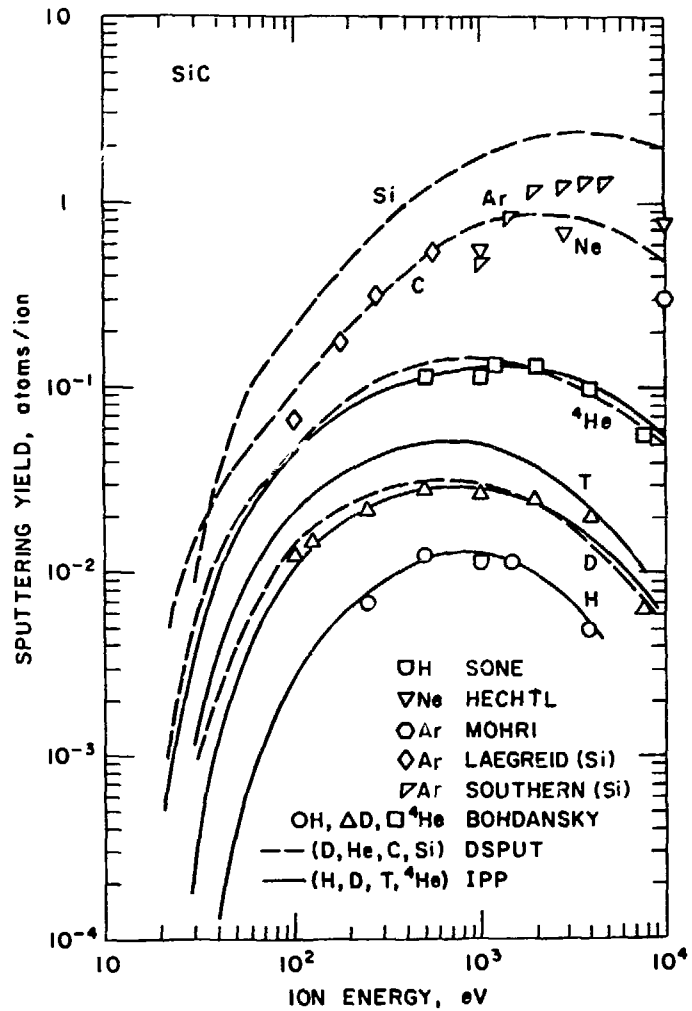

Fig. 5-2. Energy-dependent physical sputtering yields for SiC.

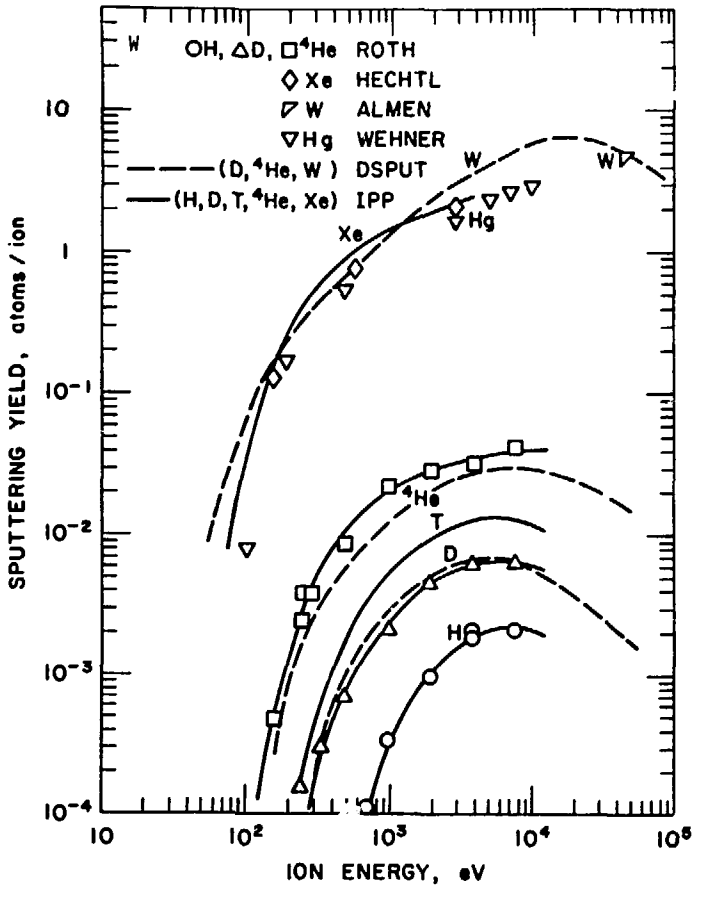

Fig. 5-3. Energy-dependent physical sputtering yields for tungsten.

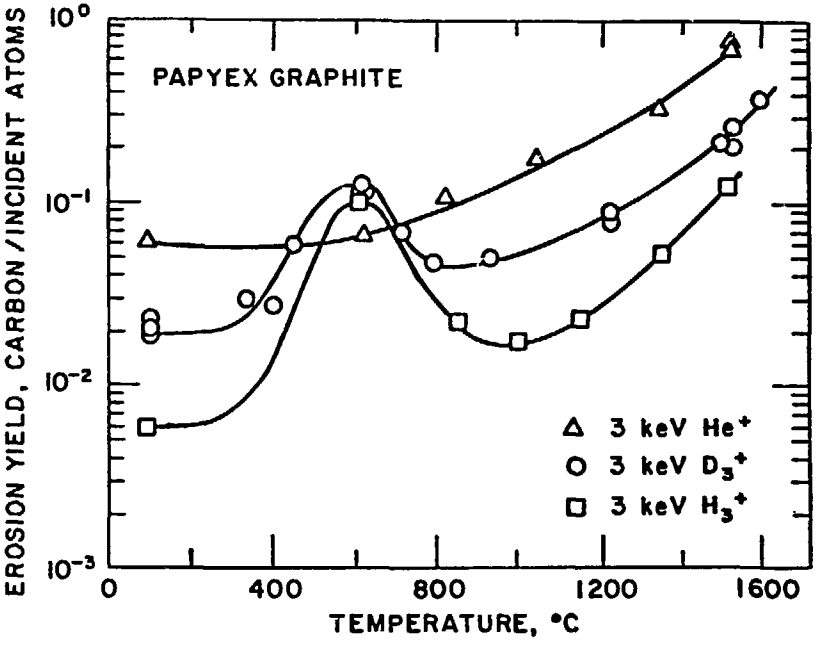

Fig. 5-4. Temperature dependence of the chemical sputtering yield of papyex graphite.

average monthly concentration. The usual methods for regulating Be concentration are the use of air filtering systems and special local pickups for dust removal at Be work stations (e.g., machining equipment). Work clothes used in Be work areas should be laundered after every shift, and the clothing should be laundered at the plant site. Respirators shall be used if the concentration exceeds 25 $\mu g/m^3$. As a final note, although special precautions are required, beryllium and beryllium containing alloys are safely used on a regular basis.

The major uncertainty with high-Z materials is the energy at which self sputtering reaches unity. Best estimates place this energy at $\sim$ 700 eV for W and Ta, but there is little experimental data in this regime. The energy at which self sputtering reaches unity is important because it determines the usable plasma edge temperatures for high-Z materials.

5.2 Heat Sink Materials

Copper alloys are the preferred heat sink materials based upon availability, fabricability, operating temperature range, and applicability to future devices. Several potential copper alloys are listed in Table 5-2. The major objective in the selection of a copper alloy is to maintain a high thermal conductivity while producing high mechanical strength. In order to maintain the thermal conductivity at a high level, the alloying concentrations for the alloys shown in Table 5-2 are kept $\lesssim$ 2.5%. High strength in these alloys is obtained by cold working and/or heat treating. In the case of those alloys whose strength is obtained primarily by cold working, there is a concern that the strength will be reduced by the high temperature procedures required for brazing or welding. Only the Cu-Be alloys offer high strength through a heat treating process alone, and they therefore have the greatest potential in this application.

5.3 Summary

The materials assessments indicate that graphite has many desirable characteristics including high thermal shock resistance, low cost, and reasonably good fabricability. It has potentially serious problems in chemical sputtering and in redeposition. The chemical sputtering can probably be controlled by maintaining the surface temperature at $\lesssim$ 400°C. However, the form and properties of redeposited graphite must be experimentally determined. If

Table 5-2
Copper Alloys Considered

Alloy Group	Typical Alloys	Composition	Remarks
Pure Copper	OFHC	99.95 - 99.99% Cu	Rather difficult to machine. Mechanical properties largely determined by degree of cold work. Mechanical strength is lost at relatively low temperatures.
Oxide Dispersion Strengthened Copper	Glidcop Al-20 Glipcop Al-60	Pure Cu + 0.15% - 0.75% Al_2O_3 depending on grade	Produced only via powder metallurgy techniques. Good mechanical and physical properties to ~ 350°C. Only limited millforms available.
Low Concentration Age-Hardened Alloys	AMSIL AMZIRC AMCROM AMAX-MZC	Pure Cu + 0.27% to 0.85% Ag Pure Cu + 0.13 - 0.20% Zr Pure Cu + 0.6% to 1.2% Cr Pure Cu + 0.03 - 0.6% Mg 0.06 - 0.15% Zr 0.04 - 0.80% Cr	Small concentrations of Ag, Zr, Mg, and Cr improve creep resistance and softening characteristics to ~ 300°C. Only limited high strength is produced by a combination of cold work and age hardening.
Be - Cu Alloy	Berylco 165 Alloy M25	Pure Cu + 0.25% - 2.0% Be 0.2% - 2.7% Co + Ni + Fe	Very high strength copper alloys available in a large variety of forms. Lowest conductivity of Cu alloys examined.

redeposited graphite has acceptable properties, then it would be the preferred surface material. Other candidate low-Z materials, Be and BeO, have safety concerns, and melt layers are predicted to form during disruptions. The preferred heat sink material is a copper alloy, but further development is required to select the best alloy.

6.0 THERMAL HYDRAULIC AND STRESS ANALYSIS

The temperatures in the limiter have been calculated. The model used for the limiter is shown in Fig. 6-1, and the assumed operating conditions are given in Table 6-1. The results, presented in Table 6-2, indicate that the surface temperatures, with the exception of SiC, are low and within acceptable limits. The required flow velocity to achieve a heat transfer coefficient of 30,000-40,000 W/m^2 K is 5-7 m/s. The coolant channel dimensions have been estimated for a total coolant flow rate of 60 kg/s. For a velocity of 3.8 m/s, the height of the channel, h, is estimated to be only 2 mm, the width, w, is 5 mm, and the rib width separating channels, b, is 3 mm. Since these dimensions are already small, it may be necessary to increase the total flow rate rather than reduce the channel size in order to increase the coolant velocity and hence the heat transfer coefficient.

The major problems for the heat sink are expected to be in the thin layer of structural material that covers the coolant channels, since this layer experiences both the highest temperatures and thermal stresses of the entire heat sink (See Fig 6-1). The temperatures, thermal stresses, and fatigue lifetimes for the top structural layer have been calculated for a heat flux of 2 MW/m^2 using a range of values for the heat transfer coefficient. The top layer has been modeled by assuming that it is totally constrained from thermal expansion by the more massive heat sink support structure to which it is bonded. As shown in Table 6-3, the value of the heat transfer coefficient is largely responsible for the operating temperatures and stresses. Fatigue is predicted to be the most restrictive property for the heat sink. The heat transfer coefficient should be $\gtrsim$ 25,000 W/m^2 K in order to achieve a fatigue lifetime of $> 10^4$ cycles. (Note: the fatigue estimates include a safety factor of two in strain or 20 in cycles to failure, whichever is lower.) In general, the copper alloys exhibit superior mechanical properties to pure

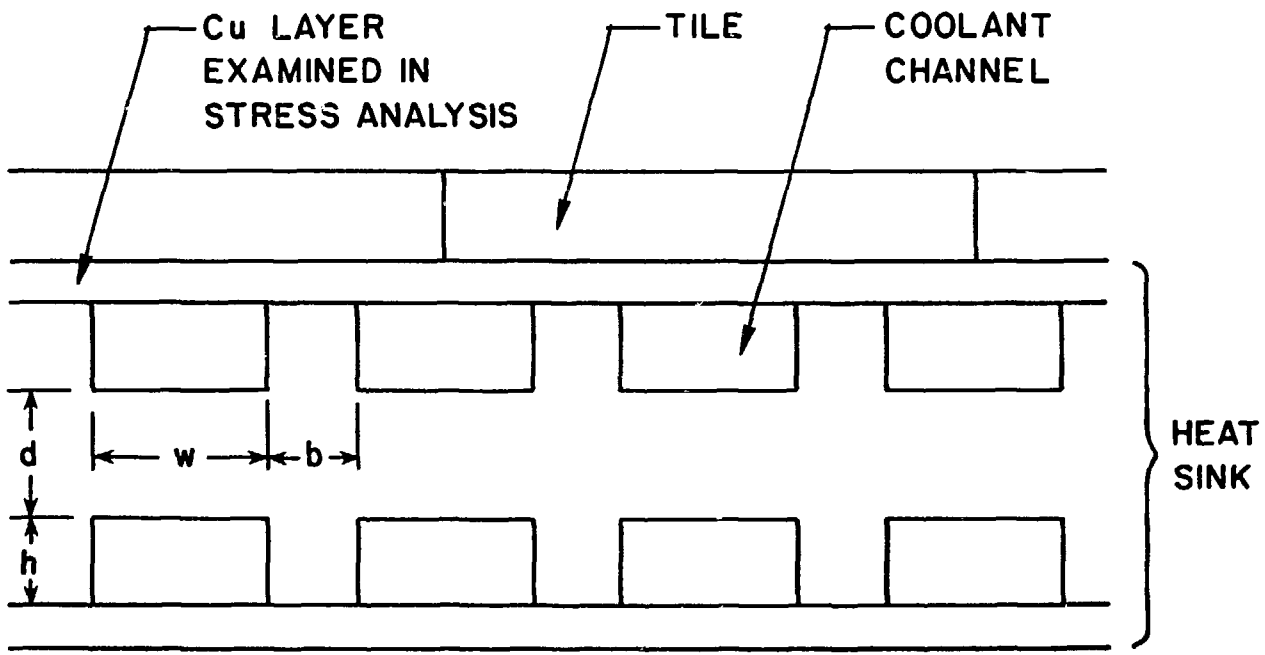

Fig. 6-1. Limiter cross section.

Table 6-1
Operating Conditions for Alcator DCT

Coolant Temperature	343 K
Heat Transfer Coefficient	40,000 W/mK
Heat Flux -	
Top	2.0 MW/m^2
Leading Edge	1.0 MW/m^2
Heat Sink	1.5 mm Cu Alloy
Plasma Side Material	C, Be, BeO, SiC, W
Thickness	1-12 mm
Thermal Conductance Between Plasma Side* and Heat Sink Material	INFINITE

* High conductance bond is required to maintain acceptably low surface temperatures.

Table 6-2
Peak Temperatures of Plasma Side Materials @ 2 MW/m^2

Material	Peak Temperature (K)				
	1 mm**	2 mm	4 mm	8 mm	12 mm
C - Top	404	419	436	489	541
LE*	371	379	388	414	439
Be - Top	401	416	440	488	538
LE	371	379	387	413	437
BeO - Top	402	414	425	463	499
LE	371	376	384	401	417
SiC - Top	443	521	678	993	1233
LE	403	431	486	603	773
W - Top	403	421	439	495	549
LE	372	380	390	418	445

* LE ≡ Leading Edge
** Plasma side tile thickness

Table 6-3.
Temperature and Mechanical Response of Limiter @ 2 MW/m^2

HT Coef. W/m^2 K**	Peak Stress* MPa	Peak Temp. K	Ultimate Strength (MPa)				Fatigue Life Cycles to Failure	
			Ann. Cu	50% CW Cu	AMAX-MZC	Cu-.5 Be	Pure Cu	Alloy
5,000	1130	750	60	60	---	457	---	1
10,000	573	553	110	150	400 (est)	786	---	72
17,500	352	468	160	330	---	842	250	4430
25,000	259	434	180	340	---	857	1.1×10^4	6.9×10^4
40,000	176	404	190	345	---	868	1.8×10^5	2.2×10^6
60,000	129	387	200	350	590	873	2.1×10^6	3.4×10^7

* Elastic stress.
** Heat transfer coefficients to ~ 40,000 W/m^2 K can be easily obtained.

copper. An estimate of the influence of heat flux on the number of cycles to failure is shown in Fig. 6-2. The fatigue lifetime is very sensitive to the surface heat flux, and for a lifetime of 10^4 cycles, the allowable heat flux is 3-4 MW/m^2. The allowable heat flux in this case is roughly proportional to the value of the heat transfer coefficient.

In summary, the flat continuous limiter appears to be well within acceptable operating limits. There are, however, other important factors to be considered. In particular, the properties and limits of bonds need to be taken into account. Also, 2-D and 3-D temperature and stress calculations will ultimately be required.

7.0 LIFETIME ANALYSIS

The lifetime of the limiter is determined by the rate of erosion, assuming that fatigue is not a concern. The erosion rate per year can be calculated from the sputtering loss rate, the disruption loss rate, and the operating schedule of Alcator DCT. The assumed operating schedule is given in Table 7-1. The estimated material loss rate for the candidate plasma side materials is given in Table 7-2. The total loss rates per year are presented in Table 7-3 for Be, BeO, C, and W. SiC has not been evaluated due to uncertainties in self sputtering. In general, the losses due to physical sputtering and redeposition are low. In the case of Be and BeO, disruption losses dominate total erosion. Graphite is attractive as a plasma side material because of the low disruption loss rate. If the edge temperature is low, then W (and Ta) is predicted to exhibit very low erosion losses. Erosion losses for SiC would also be low if self sputtering is found to be less than one.

8.0 SUMMARY AND RECOMMENDATIONS FOR ALCATOR DCT

1. The flat continuous limiter appears to be a viable impurity control system for DCT.

2. Graphite is the preferred plasma side material with qualification. It must be demonstrated experimentally that sputtered graphite particles do redeposit and that the redeposited material exhibits acceptable properties. If redeposition of graphite is not demonstrated, then Be or BeO would be preferred.

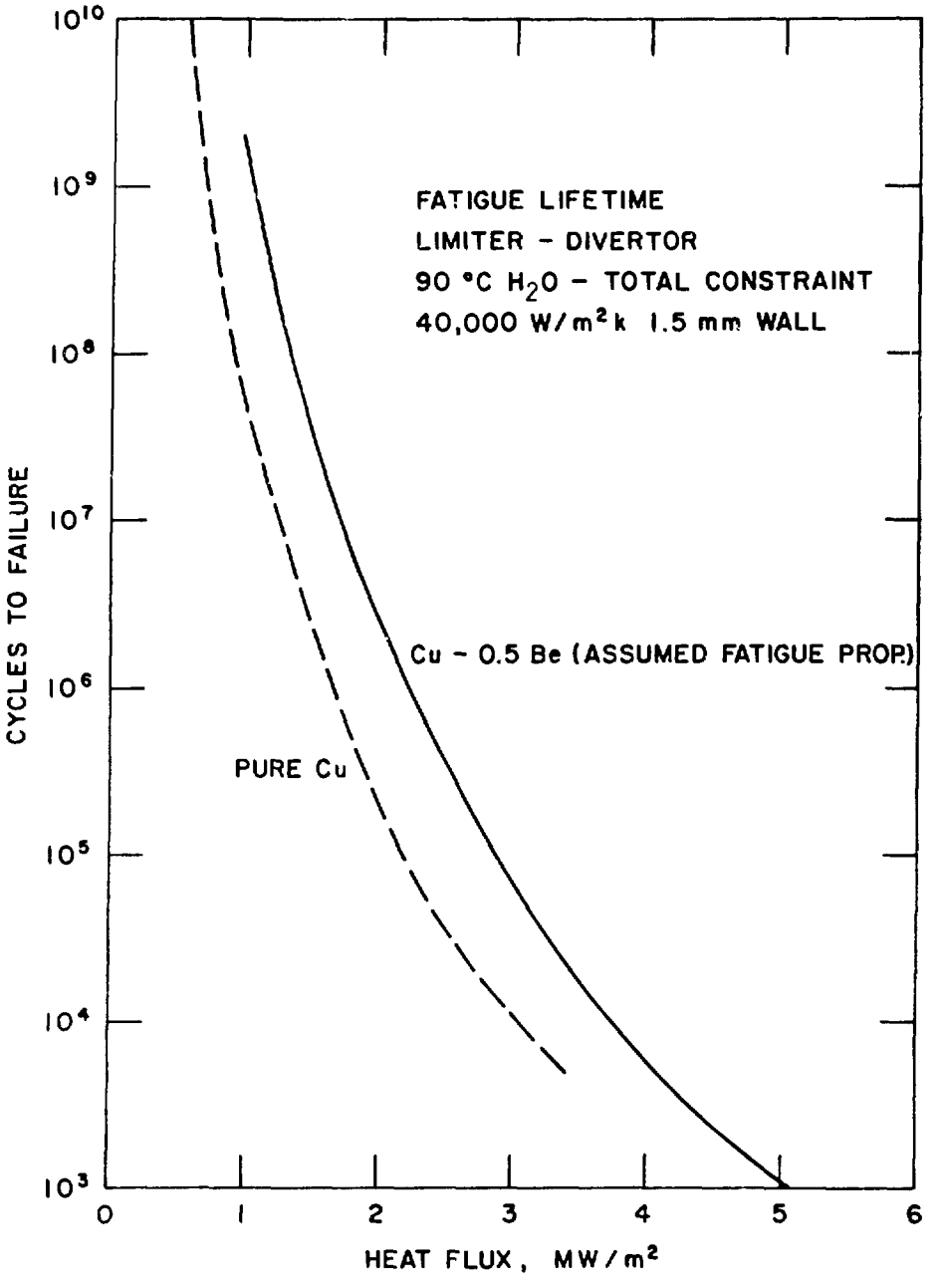

Fig. 6-2. Fatigue lifetime of the limiter heat sink as a function of heat flux.

Table 7-1
Operating Schedule Assumed for Lifetime Analysis (Per Year)

Year	Number of Shots	Total Plasma Time (s)	Number of Disruptions
1	10^4	1.0×10^5	2500
2	10^4	3×10^5	1000
3-10	1.5×10^4	1.5×10^6	300

Table 7-2
Material Erosion Rate for Candidate Plasma Side Materials

Material	Physical Sputtering	Loss Per Disruption*	
		Ref. Energy Density	2x Ref. Energy Density
C	1.6 cm/yr	0	8 μm
Be	2.7 cm/yr	46 μm	73 μm
BeO	2.7 cm/yr	18 μm	30 μm
W**	0	0	Low

* Melt layer is assumed to be eroded.

** At $T_e \lesssim 50$ eV.

Table 7-3
Erosion Rate Per Year for Candidate Plasma Side Materials

Material	Year of Operation	Erosion Rate (cm/yr)		
		Without Disruptions	Ref. Disruption	Twice Ref. Disruption Energy
Be	1	9×10^{-3}	11.5	18.2
	2	2.7×10^{-2}	4.6	7.3
	3-10	1.4×10^{-1}	1.5	2.2
BeO	1	9×10^{-3}	4.5	7.5
	2	2.7×10^{-2}	1.8	3.0
	3-10	1.4×10^{-1}	0.7	1.0
C	1	5×10^{-3}	5×10^{-3}	2.0
	2	1.5×10^{-2}	1.5×10^{-2}	0.8
	3-10	7.6×10^{-2}	7.6×10^{-2}	0.3
W*	1	0	0	Low
	2	0	0	Low
	3-10	0	0	Low

* $T_e \lesssim 50$ eV.

3. A copper alloy is preferred as the heat sink material. Considerable development is required in the areas of fabrication and bonding before the best alloy and fabrication procedures can be identified.

4. The plasma side material should be metallurgically bonded to the heat sink in order to reduce operating temperatures. This is particularly important for graphite so that the chemical sputtering regime can be avoided.

5. For a peak heat flux of 2 MW/m^2, the heat transfer coefficient between the heat sink material and the water coolant should be $\gtrsim$ 25,000 W/m^2 K to reduce thermal stresses and to increase the fatigue lifetime.

6. Assuming that the redeposition behavior of graphite is acceptable, the limiter lifetime is estimated to be high (> 5 y) for a tile thickness of 0.5 cm. Lifetimes of Be and BeO are predicted to be < 1 y due to disruption losses.

REFERENCES

(1) J. Schultz and D. B. Montgomery, "Design of the Alcator DCT Tokamak at MIT," MIT Plasma Fusion Center Report PFC/JA-83-15, 1983.

(2) B. Lipshultz, Massachusetts Institute of Technology, Personal communication.

(3) J. N. Brooks, J. Nucl. Mat. 111 & 112, (1982), p. 457.

(4) J. N. Brooks, J. Nucl. Tech-Fusion, July, 1982 (to be published).

(5) "Alcator DCT Concept Review," February 14, 1983.

(6) M. A. Abdou, et al., "US FED INTOR Critical Issues," USA FED-INTOR/82-1 (1982).

(7) D. B. Montgomery, et al., "Alcator DCT, 24 Coil Point Design Description," MIT, February, 1983.

(8) W. M. Stacey, et al., "U.S. FED-INTOR Activity and U.S. Contribution to the International Tokamak Phase-2A Workshop," USA FED-INTOR/82-1 (1982).

(9) A. M. Hassanein, et al., "Dynamics of Melting, Evaporation, and Resolidification of Materials Exposed to Plasma Disruptions," University of Wisconsin UWFDM-468 (1982).

(10) J. Roth, J. Bohdansky, and K. L. Wilson, "Chemical Erosion of Carbon Due to Bombardment with Energetic Hydrogen Ions up to 2000K," J. Nucl. Mater., 111 and 112, 775 (1982).

(11) "Beryllium," Data Sheet 562, Material Safety Council (1965).

(12) "Federal Control on Occupational Exposures to Beryllium: A Rapid-Reference Compliance Guide," Kawecki Berylco Industries, Inc. (1971).

Distribution for ANL/FPP/TM-175

Internal:

M. Abdou
C. Baker
E. Beckjord
C. Boley
J. Brooks
F. Cafasso
Y. Cha
R. Clemmer
D. Ehst
K. Evans
P. Finn
B. Frost
Y. Gohar
L. Greenwood
D. Gruen
A. Hassanein
C. Johnson
J. Jung
M. Kaminsky
S. Kim
Y-K. Kim
R. Kustom
R. Lari
B. Loomis
Y. Liu
S. Majumdar
V. Maroni
R. Mattas
B. Misra
L. Neimark
F. Nichols
J. Norem
R. Nygren
W. Praeg
J. Rest
J. Roberts
D. Smith
H. Stevens
L. Turner
R. Weeks
ANL Patent Dept.
FP Program (46)
ANL Contract File
ANL Libraries (2)
TIS Files (5)

External:

DOE-TIC, for distribution per UC-20 (108)
Manager, Chicago Operations Office, DOE
Special Committee for the Fusion Program:
S. Baron, Burns & Roe, Inc., Oradell, N.J.
H. K. Forsen, Exxon Nuclear Co., Inc., Bellevue, Wash.
M. J. Lubin, Standard Oil Co. of Ohio, Warrensville Heights, OH
G. H. Miley, U. of Illinois, Urbana, IL
P. J. Reardon, Princeton University
D. Steiner, Rensselaer Polytechnic Inst.
K. R. Symon, U. of Wisconsin-Madison
K. Thomassen, Lawrence Livermore National Lab.
B. Lipshultz, Massachusetts Institute of Technology
B. Montgomery, Massachusetts Institute of Technology
R. Parker, Massachusetts Institute of Technology
J. Schultz, Massachusetts Institute of Technology